Journal of Biomedical Optics

SPIEDigitalLibrary.org/jbo

Time-reversed ultrasonically encoded optical focusing in biological tissue

Puxiang Lai
Xiao Xu
Honglin Liu
Lihong V. Wang

SPIE

Time-reversed ultrasonically encoded optical focusing in biological tissue

Puxiang Lai, Xiao Xu, Honglin Liu, and Lihong V. Wang
Washington University in St. Louis, Department of Biomedical Engineering, Optical Imaging Laboratory, Campus Box 1097, 1 Brookings Drive, St. Louis, Missouri 63130

Abstract. We report an experimental investigation of time-reversed ultrasonically encoded optical focusing in biological tissue. This technology combines the concepts of optical phase conjugation and ultrasound modulation of diffused coherent light. The ultrasonically encoded (or tagged) diffused light from a tissue sample is collected in reflection mode and interferes with a reference light in a photorefractive crystal (used as a phase conjugation mirror) to form a hologram. Then a time-reversed copy of the tagged light is generated and traces back the original trajectories to the ultrasonic focus inside the tissue sample. With our current setup, we can achieve a maximum penetration depth of 5 mm in a chicken breast sample and image optical contrasts within a tissue sample with a spatial resolution approximately equaling $1/\sqrt{2}$ of the ultrasound focal diameter. [DOI: 10.1117/1.JBO.17.3.030506]

Keywords: optical imaging; optical focusing; ultrasound modulation; optical phase conjugation; time reversal; photorefractive crystal; reflection mode; biological tissue.

Paper 11563 received Sep. 30, 2011; revised manuscript received Jan. 20, 2012; accepted for publication Jan. 23, 2012; published online Mar. 8, 2012; corrected Mar. 19, 2012.

The spatial resolution of optical imaging at depths beyond one transport mean free path (typically ~1 mm in scattering tissue) is compromised by the multiple scattering of light in biological tissue.[1] Therefore, methods to efficiently focus or deliver light tightly into tissue relatively deeply are intensively explored. Among them, spatial wavefront shaping [2,3] and optical phase conjugation (OPC)[4,5] are promising in "suppressing" the turbidity of media. The former approach uses a spatial light modulator to optimize the relative phases of the segments of an incident beam's wavefront pattern and a feedback algorithm to maximize the resultant light intensity at a desired focal point beyond[3] or inside[6] a turbid medium. In both cases, the transmitted segments interfere constructively at the focal point. The latter approach, OPC, employs a phase conjugation mirror (PCM) to generate a phase conjugated wavefront of the diffused light from a turbid medium. Due to the reciprocity of light propagation, the conjugated wavefront travels back through the turbid medium and refocuses where the observer has direct optical access. The feasibility of focusing using OPC has been demonstrated with both diffusive phantoms and biological tissue.[5,7] However, the refocused site in this approach has to be outside the turbid medium. This limitation hinders OPC's use in broad and practical applications.

Most recently, Xu et al.[8] introduced a focused ultrasonic beam as an internal "guide star" for OPC, so that the resultant optical focal point can be positioned anywhere inside a turbid medium. In this technique, called time-reversed ultrasonically encoded (TRUE) optical focusing, a turbid medium is exposed simultaneously to coherent incident light and a focused ultrasound field. The incident photons experience a series of random elastic scattering events within the sample. Part of the scattered photons traverse the ultrasound region, i.e., the acousto-optic (AO) interaction volume, and are "tagged" with an ultrasonic frequency.[9] The resultant diffused light, collected outside the sample, is sent to a photorefractive crystal (PRC) functioning as a PCM. Unlike the general OPC method, in TRUE optical focusing, only the ultrasonically tagged photons contribute to a stable hologram, which later generates a time-reversed wavefront. Since all tagged photons originate from the AO interaction volume, the conjugated copy will eventually travel back, although tortuously, to the AO interaction volume inside the turbid medium. Given the much broader spatial distribution of the diffused light, the ultrasound focus determines the AO interaction volume, hence the location and extent of the "time-reversed" focus. Therefore by moving the relative position of the ultrasound focus inside the turbid medium, one can dynamically focus light to anywhere predefined by the ultrasound focus.

TRUE optical focusing in turbid media was first implemented in transmission mode, where light incidence and collection are on opposite sides of the turbid medium.[8,10] To make this concept more practical and convenient for biomedical application, a reflection mode configuration has been developed by installing the optical delivery and collection components on the same side of a sample.[11] With this setup, a round-trip optical focusing path length up to 160 mean free paths has been attained. In these earlier studies, tissue mimicking phantoms made of porcine gelatin gel doped with intralipid were used as turbid media. The phantoms were easily fabricated, with controllable geometries, homogeneities, and other physical properties, but they could not duplicate some characteristics of real biological tissue, such as acoustic attenuation ($0.04\,\mathrm{dB\,cm^{-1}\,MHz^{-1}}$ for 10% gelatin phantom[12] versus $0.75\,\mathrm{dB\,cm^{-1}\,MHz^{-1}}$ for regular human breast tissue[13]) and multiscale microstructures. In this work, we report the first experimental exploration of TRUE optical focusing in biological tissue.

Figure 1 shows the system configuration, where a 532-nm continuous-wave laser (frequency) was split into three beams: a signal beam (S), a reference beam (R), and a phase conjugated reading beam (R^*). During the hologram writing phase (0 to 190 ms), S illuminated a tissue sample with its frequency shifted by f_a due to two AO modulators functioning in series. Inside the sample, photons were multiply scattered, and those traversing the ultrasound focal region were frequency shifted by $\pm f_a$ in the AO interaction volume. The resultant back-scattered optical field, after being transmitted through a high numerical aperture light guide, interfered with R in a

Address all correspondence to: Lihong V. Wang, Washington University in St. Louis, Department of Biomedical Engineering, Optical Imaging Laboratory, Campus Box 1097, 1 Brookings Drive, St. Louis, Missouri 63130. Tel: (314) 935-6152; Fax: (314) 935-7448; E-mail: lhwang@biomed.wustl.edu

0091-3286/2012/$25.00 © 2012 SPIE

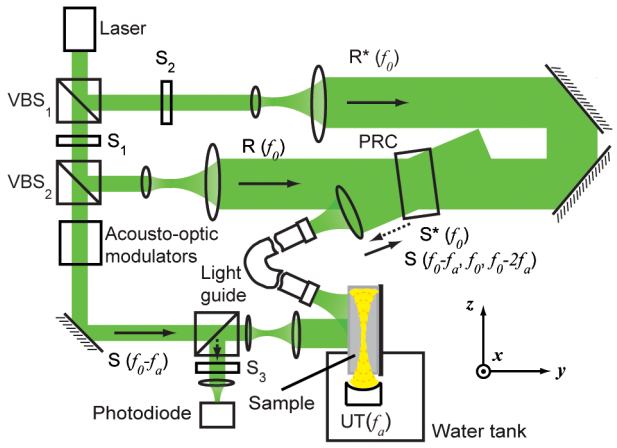

Fig. 1 System schematic. The component labels are defined as follows: VBS_{1-3}, variable beam splitters, each composed of a half-wave plate and a polarizing beam splitter; S_{1-3}, shutters; UT, ultrasound transducer; PRC, photorefractive crystal; f_0, frequency of laser; f_a, frequency of ultrasound; $S(f_0 - f_a)$, light incident on the sample; $S(f_0 - f_a, f_0, f_0 - 2f_a)$, reflectively collected diffused light from the sample; $R(f_0)$, the reference beam; $R^*(f_0)$, the conjugate reading beam; $S^*(f_0)$, the time-reversed copy of ; *xyz*, system coordinates (*y* is the optical illumination direction, and *z* is the ultrasound propagation direction).

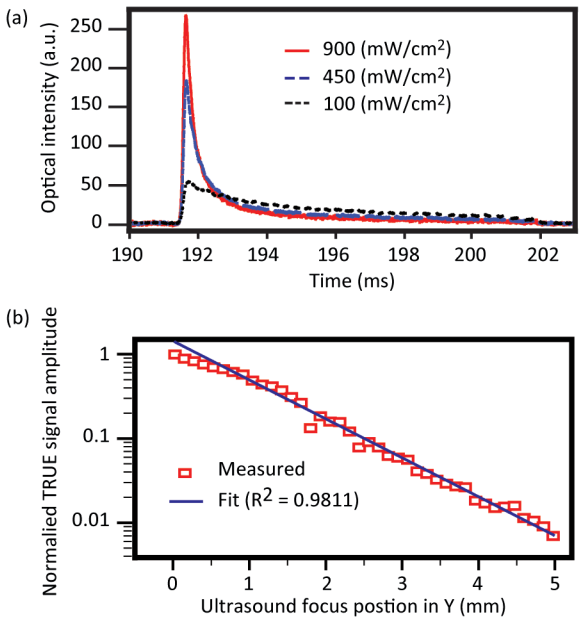

Fig. 2 (a) Examples of averaged TRUE signals obtained in a tissue sample under various reading beam intensities. (b) Normalized TRUE signal amplitude as a function of ultrasound focal position along the *y* direction.

$Bi_{12}SiO_{20}$ (BSO) PRC. The only stationary interference pattern was formed by the photons with the same frequency, f_0. The recording time of 190 ms was determined by the characteristics of the PRC and the interfering beams' intensities. In the subsequent window from 190 to 200 ms, S and R were blocked, and R^* illuminated the PRC along the direction opposite to R and instantly generated a "time-reversed" wavefront $S^* \cdot S^*$ backtraced the original trajectories into the tissue sample and eventually converged to the ultrasound focus. Throughout this work, ultrasound waves with a central frequency of 3.5 MHz, a full width at half maximum (FWHM) focal width of 0.87 mm, and a focal pressure of 1.33 MPa (peak-to-peak) were used. Further details about the system and its operation can be found in the literature.[8,11]

It should be highlighted that the validity of "time reversal" requires that the system, including the experimental sample, remain stationary during the whole process of hologram recording and reading. Therefore, the PCM should operate sufficiently fast with respect to the system's decorrelation time, a function determined by the tissue's micro-physiological motion (~1 ms for *in vivo* biological tissue,[14] depending on the depth), optical element vibration, and ambient disturbance. Limited by the response time of the PCM currently used (on the order of tens of ms), in this study we focused only on *ex vivo* chicken breast tissue, but we are mindful that *in vivo* soft biological tissue is the ultimate intended medium for this technique. As shown in Fig. 1, the chicken breast sample was partially submerged in water in the z direction, while the position of the ultrasound focus was above the water surface. To ensure good acoustic coupling at the tissue-air and water-air interfaces when the ultrasound wave was very close to the y boundaries of the tissue slab ($y = 0$ on the left), the tissue slab was sandwiched between two layers of transparent porcine gelatin gel.

Figure 2(a) shows three example TRUE signal waveforms (averaged 32 times) obtained from a tissue sample when the ultrasound focus was placed at depth $y = 0.5$ mm, each corresponding to a different optical intensity of R^*, while all the other experimental conditions were kept identical. Note that the artifacts caused by the scattered reading beam in the photodiode output had already been removed.[11] Although R^* was allowed to illuminate the sample at $t = 190$ ms, there was no time-reversed signal until approximately $t = 191.5$ ms due to the response delay and opening speed of S_2. The hologram right after $t = 191.5$ ms was erased by R^*, rendering a sharp TRUE response peak that decayed rapidly afterwards. Since the erasure time constant of a recorded hologram in a PRC is inversely proportional to the illumination intensity,[15] increasing the intensity of R^* resulted in a higher amplitude of R^*, but also a faster erasure of the hologram, i.e., a shorter TRUE signal. Hence a more intense reading beam is usually preferred. For the safety of the optical components, R^* in our study was limited to 900 mW/cm^2.

The amplitude of the TRUE signal also depends on the strength of the recorded hologram, which in turn is a function of the ultrasound field and its position inside the sample, the optical properties of the medium, and other factors. Figure 2(b) shows the normalized TRUE signal amplitude as a function of the ultrasound focal position scanned along the y direction, while all other experimental conditions remained constant. At each position, the amplitude of a TRUE signal was obtained. The exponential decay of the TRUE signal amplitude (shown in squares) with y is evident. A fit for y positions sufficiently away from the tissue front surface (starting from $y = 0.635$ mm) yielded an exponential decay rate of 1.02 mm^{-1}, with a fitting coefficient of determination $R^2 = 0.9811$. Considering the round-trip optical path in the reflection mode, the TRUE signal amplitude actually decayed exponentially at a rate of $1.02/2 = 0.51$ mm^{-1}. This value is close to the effective attenuation coefficient ($\mu_{\text{eff}} = \sqrt{3\mu_a(\mu_a + \mu_s')}$, a parameter governing the fluence decay rate of diffused light) of regular *ex vivo* breast tissue at 532 nm.[16] This slow decay rate confirms that TRUE optical focusing is capable of suppressing the medium's turbidity by converging multiply scattered photons, instead of ballistic photons, back into the encoded region inside a tissue sample. A maximum penetration depth of 5 mm,

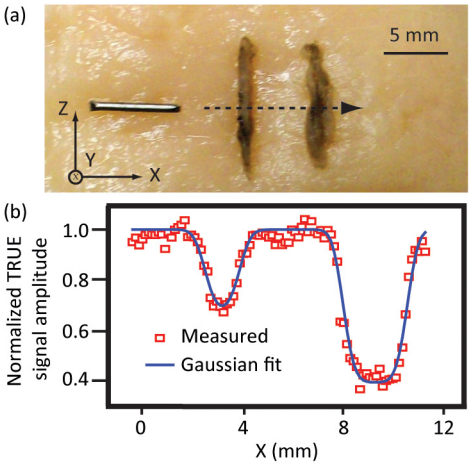

Fig. 3 (a) Tissue sample cross-section. Two India ink-dyed tissue pieces are embedded as absorption objects. (b) Normalized TRUE signal amplitude distribution when the tissue sample is scanned along the x direction.

equivalent to about 100 mean free paths for a round trip, has been obtained with the current setup.

To study the spatial resolution of TRUE optical focusing in tissue, two small tissue pieces were dyed with India ink as optical absorption objects and embedded 2.5 to 3.0 mm deep inside a large tissue sample. A photograph of the cross-section of the sample is shown in Fig. 3(a), where the needle on the left was used to ensure the ultrasound focus coincided with the objects in both y and z directions. During the experiment, the tissue sample was scanned along the x direction while the light and the ultrasound remained stationary. The TRUE signal amplitude was obtained at each x position, and its distribution is plotted in Fig. 3(b) (shown in squares) as a function of the sample's x position. Because TRUE optical focusing directs light tightly back to the AO interaction volume, whenever this interaction volume scans across an object having a higher optical absorption than the background, the TRUE signal amplitude is reduced due to the decrease in the number of ultrasound modulated photons. Through such a contrast mechanism, the embedded objects can be imaged out of the background, as shown in Fig. 3(b). A Gaussian fit was applied to the data, from which the position and dimension of the objects could be determined: 0.75 mm wide for the left object at $x = 3.5$ mm with a negative contrast of 32%, and 1.20 mm wide for the right object at $x = 9.6$ mm with a negative contrast of 60%. The 1D image agrees well with the photograph shown in Fig. 3(a). The FWHM of the TRUE focus computed from the Gaussian fit is 0.67 mm, approximating $1/\sqrt{2}$ of the ultrasound focal width (0.87 mm) and consistent with the square law.[8]

In summary, we report the first experimental exploration of TRUE optical focusing in biological tissue. We show that TRUE is able to efficiently suppress tissue turbidity and dynamically focus light into tissue at depths up to 5 mm while maintaining a small focal region defined by the ultrasound focus. In comparison with phantoms,[11] tissue has higher attenuation for both light and sound. Consequently, less maximum optical penetration can be obtained, even though enhanced ultrasound modulation is employed. The PRC in current system requires a relatively long time for hologram writing, and thus it restrains the investigation to *ex vivo* tissue. A faster PRC (with sub-millisecond response time) needs to be employed in future studies to overcome the system decorrelation limit caused by tissue internal motion *in vivo*.

Acknowledgments

This research is sponsored in part by the National Academies Keck Futures Initiative grant IS 13 and the National Institute of Health through grants R01 EB000712 and U54 CA136398. L.W. has a financial interest in Microphotoacoustics, Inc. and Endra, Inc., which, however, did not support this work.

References

1. L. V. Wang and H. Wu, *Biomedical Optics: Principles and Imaging*, John Wiley and Sons, Hoboken, NJ (2007).
2. W. B. Bridges et al., "Coherent optical adaptive techniques," *Appl. Opt.* **13**(2), 291–300 (1974).
3. I. M. Vellekoop and A. P. Mosk, "Focusing coherent light through opaque strongly scattering media," *Opt. Lett.* **32**(16), 2309–2311 (2007).
4. R. A. Fisher, Ed., *Optical Phase Conjugation*, Academic Press, New York (1983).
5. Z. Yaqoob et al., "Optical phase conjugation for turbidity suppression in biological samples," *Nat. Photonics* **2**(2), 110–115 (2008).
6. I. M. Vellekoop et al., "Demixing light paths inside disordered metamaterials," *Opt. Express* **16**(1), 67–80 (2008).
7. E. J. McDowell et al., "Turbidity suppression from the ballistic to the diffusive regime in biological tissue using optical phase conjugation," *J. Biomed. Opt.* **15**(2), 025004 (2010).
8. X. Xu, H. Liu, and L. V. Wang, "Time-reversed ultrasonically encoded optical focusing into scattering media," *Nat. Photonics* **5**(3), 154–157 (2011).
9. L. V. Wang, "Mechanisms of ultrasound modulation of multiply scattered coherent light: an analytic model," *Phys. Rev. Lett.* **87**(4), 043903 (2001).
10. H. Liu et al., "Time-reversed ultrasonically encoded (TRUE) optical focusing into tissue-mimicking media with optical thickness up to 70," *J. Biomed. Opt.* **16**(8), 086009 (2011).
11. P. Lai et al., "Reflection-mode time-reversed ultrasonically encoded (TRUE) optical focusing into turbid media," *J. Biomed. Opt.* **16**(8), 080505 (2011).
12. J. R. Cook, R. R. Bouchard, and S. Y. Emelianov, "Tissue-mimicking phantoms for photoacoustic and ultrasonic imaging," *Biomed. Opt. Express* **2**(11), 3193–3206 (2011).
13. F. A. Duck, *Physical Properties of Tissue*, Academic Press, San Diego (1990).
14. M. Gross et al., "Detection of the tagged or untagged photons in acousto-optic imaging of thick scattering media by photorefractive adaptive holography," *Eur. Phys. J. E* **28**(2), 173–182 (2009).
15. L. Solymar, D. J. Webb, and A. G. Jepsen, *The Physics and Applications of Photorefractive Materials*, Clarendon Press, Oxford (1996).
16. J. Kolzer et al., "Measurement of the optical properties of breast tissue using time-resolved transillumination," *Proc. SPIE* **2326**, 143–152 (1995).